



Immobilization of glucose oxidase on rod-like and vesicle-like mesoporous silica for enhancing current responses of glucose biosensors

Guowei Zhou^{a,b,1}, Ka Kei Fung^{a,1}, Ling Wai Wong^a, Yijian Chen^a, Reinhard Renneberg^a, Shihe Yang^{a,*}

^a Department of Chemistry, William Mong Institute of Nano Science and Technology, The Hong Kong University of Science and Technology, Clear Water Bay, Kowloon, Hong Kong

^b Shandong Provincial Key Laboratory of Fine Chemicals, School of Chemical Engineering, Shandong Institute of Light Industry, Jinan 250353, PR China

ARTICLE INFO

Article history:

Received 15 September 2010

Received in revised form 13 January 2011

Accepted 21 January 2011

Available online 28 January 2011

Keywords:

Mesoporous materials

Rod-like SiO₂

Vesicle-like SiO₂

Glucose oxidase immobilization

Biosensor

ABSTRACT

The use of rod-like and vesicle-like mesoporous SiO₂ particles for fabricating high performance glucose biosensors is reported. The distinctively high surface areas of mesoporous structures of SiO₂ rendered the adsorption of glucose oxidase (GOx) feasible. Both morphologies of SiO₂ enhanced the sensitivities of glucose biosensors, but by a factor of 36 for vesicle-like SiO₂ and 18 for rod-like SiO₂, respectively. The greater enhancement of vesicle-like SiO₂ can be accounted for by its higher specific surface area (509 m² g⁻¹) and larger total pore volume (1.49 cm³ g⁻¹). Interestingly, the current responses of GOx immobilized in interior channels of the mesoporous SiO₂ were enhanced much more than those of simple mixtures of GOx and the mesoporous SiO₂. This suggests that the enhancement of current responses arise not only from the high surface area of SiO₂ for high enzyme loading, but also from the improved enzyme activity upon its adsorption on mesoporous SiO₂. Also compared were the performances of glucose biosensors with GOx immobilized on mesoporous SiO₂ by physical adsorption and by covalent binding to 3-aminopropyltrimethoxysilane (APTMS) modified SiO₂ using glutaraldehyde as the cross-linker. The covalent binding approach resulted in higher enzyme loading but lower current sensitivity than with the physical adsorption.

© 2011 Elsevier B.V. All rights reserved.

1. Introduction

In 1992, the Mobil research group first reported on the synthesis of mesoporous molecular sieves from the calcinations of aluminosilicate gels [1]. Since then, different types of mesoporous silicas (MPs) have been developed [2–6]. Because of the high chemical and thermal stability, low toxicity and high mechanical strength, large pore diameters (2–40 nm), matching the size of the enzymes, narrow pore size distribution, large pore volumes (ca. 1.5 cm³ g⁻¹) and high surface area (up to 1500 m² g⁻¹). MPs have been found to be a good biocompatible solid support for immobilizing enzymes [7]. The first immobilization of enzymes onto mesoporous silica MCM-41 was reported by Diaz and Balkus [8]. After that great attention has been devoted to the use of these inorganic materials for the enzyme immobilization [9–13].

Many nanomaterials have been harnessed to fabricate glucose biosensors with high sensitivity and excellent reproducibility, such as Au nanoparticles [14–17], Ag nanoparticles [18–21], Ni nanoparticles [22], carbon nanotubes [23–26], SiO₂ nanoparticles

[27–31] and mesocellular carbon foam [32]. Among these developments, the stabilized enzyme activity in MPs renders their potential applications in various fields such as biosensors [33,34,27,35,36], fuel cells [37] and enzyme-linked immunosorbent assay (ELISA) [38]. Recently, our group has successfully synthesized mesoporous rod-like silica and vesicle-like silica and applied them for immobilization of lipase with retained activity [12]. The rod-like and vesicle-like SiO₂ have large pore sizes (~11–12 nm) and abundant micropores (less than 2 nm) in the silica walls of the mesoporous rod-like and vesicle-like structure. With the success in the immobilization of lipase on these MPs, it is expected that glucose oxidase (GOx), which is also a globular enzyme, can be immobilized onto the MPs as well and further applied to the development of a glucose biosensor.

Up to now, to the best of our knowledge, there have been no comparative studies on the adsorption of glucose oxidase (GOx) onto the mesoporous rod-like and vesicle-like SiO₂ and also their applications to the electrochemical biosensors. Capitalizing on our recent success in the controlled synthesis of mesoporous silica, we aim to compare the adsorption characteristics of GOx onto the mesoporous SiO₂ with different morphologies, namely, the rod-like silica and the vesicle-like silica. We have also explored the fabrication of glucose biosensors with different modes of GOx adsorption on the mesoporous SiO₂ interior surfaces on the current responses of the glucose biosensors.

* Corresponding author. Tel.: +852 2358 7362.

E-mail addresses: guoweizhou@hotmail.com (G. Zhou), chsyang@ust.hk (S. Yang).

¹ These authors contributed equally to this work.

2. Experimental

2.1. Materials and reagents

Triblock copolymer poly(ethylene oxide)-block-poly(propylene oxide)-block-poly(ethylene oxide) (Pluronic P123, $\text{EO}_{20}\text{PO}_{70}\text{EO}_{20}$, $M_w = 5800$), tetraethoxysilane (TEOS), 3-aminopropyltrimethoxysilane (APTMS), glucose oxidase (GOx, EC 1.1.3.4, 197 U mg^{-1} solid, from *Aspergillus niger*), β -D-glucose and polyvinyl butyral (PVB) were purchased from Aldrich. 1,3,5-Triisopropylbenzene (TIPB) was purchased from Fluka. All other chemicals used in this work were of analytical reagent grade. All the chemicals were used without further purification.

2.2. Synthesis of mesoporous rod-like and vesicle-like SiO_2

Rod-like and vesicle-like SiO_2 were synthesized by simply changing the molar ratio of TIPB with P123 surfactant according to the method described in literature [5]. First, 1.0 g of P123 was dissolved in a mixture of 8.5 g of H_2O and 30 g of 2 M HCl aqueous solution and the resulting solution was stirred at room temperature until the solution became clear. Into the solution specified amounts of TIPB (with the molar ratio of TIPB:P123 being 2.9:1 and 34.8:1, respectively) were added drop-wise for the preparation of a set of samples. The mixture was stirred at room temperature for another 18 h. Secondly, 2.1 g of TEOS was added into this solution under stirring for 8 min and the mixture was kept under static conditions at 35°C for 24 h. This mixture solution was then transferred into a Teflon-lined autoclave and heated to and kept at 130°C for 24 h. Finally, white precipitates were filtered, washed with water, air-dried at room temperature, and calcined at 500°C for 6 h in a tube furnace to remove the organic templates.

2.3. Surface modification of mesoporous vesicle-like SiO_2 with amine groups

The amine functionalized mesoporous vesicle-like SiO_2 was prepared by a post-synthesis method [39,40]. The mesoporous SiO_2 was dried at 100°C for 24 h to thoroughly remove water. Amine groups ($-\text{NH}_2$) were grafted onto the mesoporous SiO_2 by refluxing 0.1 g of SiO_2 in 50 ml dry toluene (99.5%) solution containing 0.1 M APTMS at 120°C for 18 h. The suspension was then centrifuged and washed thoroughly with toluene and water in succession. The NH_2 -modified mesoporous vesicle-like SiO_2 with amine group is denoted as $\text{SiO}_2\text{-NH}_2$.

2.4. Immobilization of GOx onto mesoporous rod-like and vesicle-like SiO_2

For physisorption of GOx onto mesoporous SiO_2 , GOx was first dissolved in potassium acetate–acetic acid (KAc–HAc) buffer (pH 4.0) to obtain a GOx stock solution with a concentration of 4 mg ml^{-1} . 1 ml of KAc–HAc buffer was added to 4 mg of mesoporous SiO_2 support in 10 ml capped vials. After the mixture was sonicated for 20 min, 1 ml of the GOx stock solution was added. The total volume and concentration of GOx solution were 2 ml and 2 mg ml^{-1} . The mixture was kept stirring at room temperature for 48 h. The supernatant was separated from the solid material by centrifugation (12,000 rpm, 8 min, 4°C). The excess GOx was removed by washing with KAc–HAc buffer (pH 4.0, 1 ml), and the solid materials was dried overnight under vacuum at room temperature and then stored at 4°C . The amount of GOx adsorbed onto the mesoporous SiO_2 was further quantified by measuring the absorbance of the supernatant at 280 nm. For physisorption, the adsorbed GOx amounts were 366 and 430 mg g^{-1} for rod-like and vesicle-like SiO_2 , respectively. For covalent linking of GOx onto

the mesoporous SiO_2 , 500 μl of 1% glutaraldehyde was first mixed with 4 mg of $\text{SiO}_2\text{-NH}_2$ and the mixture was incubated for 1 h. The activated $\text{SiO}_2\text{-NH}_2$ was collected by centrifugation and washed with water, followed by incubation with 2 ml of 2 mg ml^{-1} GOx solution for 24 h. The suspension was separated by centrifugation and the solid material was washed thoroughly and then stored at 4°C . For chemisorption, the adsorbed GOx amount on $\text{SiO}_2\text{-NH}_2$ was 475.7 mg g^{-1} .

2.5. Characterization

High resolution transmission electron microscopy (HRTEM) was performed using a JEOL 2010 electron microscope. Samples for HRTEM measurements were prepared by dipping a carbon-coated copper grid into a suspension of ground samples in ethanol, which were pre-sonicated for 20 min. Field emission scanning electron microscope (FESEM) measurements were carried out with a JEOL JSM-6700F microscope. Samples were deposited on the surface of silicon wafer by dropping a suspension of ground samples in ethanol that was pre-sonicated for 20 min, and sputter coated for 2 cycles with gold. Nitrogen adsorption–desorption isotherms were measured at -196°C on a SA3100 surface area and pore size analyzer. Samples were degassed in a vacuum at 200°C for 3 h prior to each measurement, while the GOx loaded samples were outgassed at 35°C for 12 h. Brunauer–Emmett–Teller (BET) method was utilized to calculate the specific surface areas (S_{BET}) from the adsorption data. Pore size distributions were derived from the adsorption branches of isotherms by using the Barrett–Joyner–Halenda (BJH) model. The presence of functional groups in APTMS modified mesoporous SiO_2 was identified using Fourier Transform Infrared Spectroscopy (FT-IR). The FT-IR spectra were taken on KBr disks with Perkin Elmer Spectrum One USA and scanned from 400 cm^{-1} to 4000 cm^{-1} at a resolution of 4 cm^{-1} .

2.6. Fabrication of enzyme modified electrodes

Mesoporous SiO_2 imbedded with GOx was fabricated on to electrodes by sol–gel technique according to the literature [19,28]. A platinum electrode ($d = 1.5 \text{ mm}$) was first polished mechanically with an Al_2O_3 slurry ($0.03 \mu\text{m}$) and then sonicated in deionized water for 20 min until a mirror-like surface was achieved. The above prepared SiO_2 immobilized GOx (4 mg SiO_2 containing 1.464, 1.72 and 1.9028 mg GOx for rod-like SiO_2 , vesicle-like SiO_2 and $\text{SiO}_2\text{-NH}_2$, respectively) was re-suspended in 300 μl KAc–HAc buffer. Twenty microliters of the mixture suspension containing 10 μl of $\text{SiO}_2\text{-GOx}$ in KAc–HAc buffer, 10 μl of 2% PVB ethanol solution and 0.05% of glutaraldehyde was deposited onto the electrode surface and allowed to form a thin film after drying at ambient conditions. At last, the GOx modified electrode was dip-coated with one layer of PVB and then was stored at 4°C prior to use. For the sake of comparison, the electrodes modified with free GOx or mixtures of GOx and mesoporous SiO_2 were prepared as follows. The same amount of enzyme was first dissolved into 300 μl KAc–HAc buffer and then 4 mg mesoporous SiO_2 was suspended into the solution. The other steps were the same as mentioned above. The amounts of used enzyme in modified electrodes were 0.0488, 0.0573 and 0.0634 mg for rod-like SiO_2 , vesicle-like SiO_2 and $\text{SiO}_2\text{-NH}_2$, respectively. The amount of mesoporous SiO_2 in modified electrodes was 0.1333 mg .

2.7. Amperometric and cyclic voltammetry (CV) measurement

Electric current signals were measured and recorded with a potentiostat (Biometra EP-30, Göttingen, Germany). Measurements were carried out inside a stirring cell filled with 5 ml of 0.1 M phosphate buffer (pH 7.0, containing 0.1 M KCl). A three-

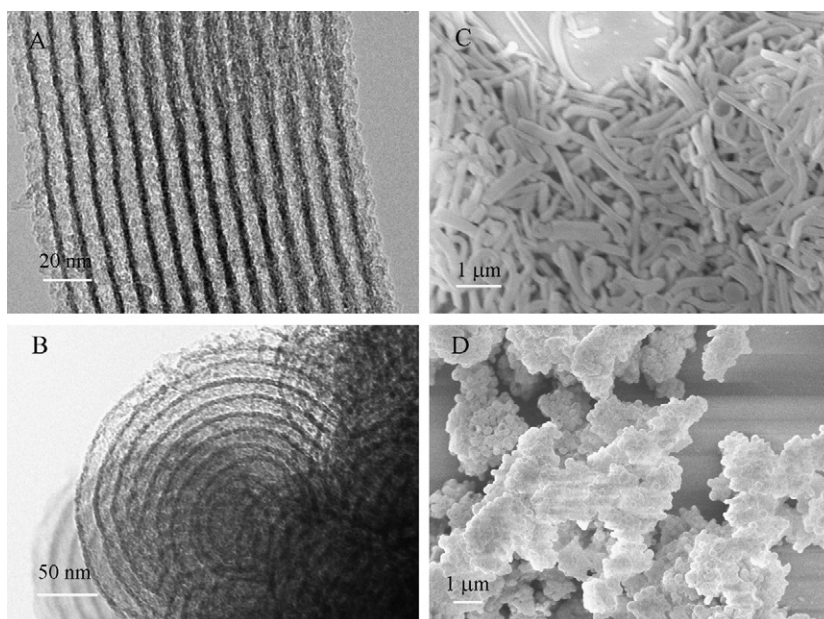


Fig. 1. Representative HRTEM and FESEM images of rod-like SiO₂ (A and C) and vesicle-like SiO₂ (B and D).

electrode configuration consisting of a surface-modified platinum working electrode, an Ag/AgCl reference electrode, and a platinum counter electrode was employed for amperometric measurements at a fixed potential of +600 mV. The electrodes were immersed in a blank buffer solution for a few minutes until a stable current was reached. β -D-Glucose solutions of different concentrations were then injected into the measurement cell, and the response current rapidly reached a new stable level. All of the experiments were conducted at room temperature and repeated three times.

Cyclic voltammetry (CV) measurement was performed by using a BAS model 100B (West Lafayette, IN) voltammetric analyzer driven by BAS 100W version 2.0 software. Three-electrode configuration was used which was the same as for amperometric measurement. Electrolyte solution was 0.1 M phosphate buffer pH 7.0, scan rate 100 mV s⁻¹, scan range 0–600 mV.

3. Results and discussion

3.1. Morphologies of mesoporous SiO₂

Representative HRTEM and FESEM images are shown in Fig. 1. Clearly contrasting are the rod-like (Fig. 1A and C) and vesicle-like (Fig. 1B and D) morphologies of the mesoporous SiO₂. As shown in Fig. 1A, the mesoporous rod-like silica (SBA-15) contains hexagonal channels ca. \sim 11 nm in diameter. On the other hand, the mesoporous vesicle-like silica (Fig. 1B) bears multilamellar channels with a size of ca. \sim 12 nm. Both of the mesoporous silica materials have SiO₂ walls ca. \sim 5 nm thick. Fig. 1D presents the aggregation of vesicle-like silica spheres. Evidently, the mesopores of such mesoporous silica materials are sufficiently large for the encapsulation of GOx molecules with a dimension of 6.0 nm \times 5.2 nm \times 3.7 nm.

3.2. Characteristics of mesoporous SiO₂ functionalized with APTMS

For covalent modification of the mesoporous silica, the methoxyl group of APTMS was allowed to react with the silanol groups on the internal surface, leaving the aminopropyl groups attached to the internal surfaces of the mesoporous SiO₂ materials. FT-IR was used to confirm the surface modification. Before the sur-

face modification, an intense adsorption band at \sim 3450 cm⁻¹ due to the stretching vibration of surface hydroxyl groups was detected, indicating the presence of abundant free silanol groups on the mesoporous SiO₂ surfaces (Fig. 2a). For the functionalized mesoporous vesicle-like SiO₂ (Fig. 2b), there is an infrared absorption band at about \sim 1570 cm⁻¹, which can be assigned to the N–H asymmetric bending of amine groups [41]. Moreover, the occurrence of a weak absorption band at \sim 2935 cm⁻¹ is thought to arise from the asymmetric stretching vibration of CH₂ of the propyl group. These results give evidence that the vesicle-like SiO₂ surfaces have been successfully functionalized by the amine groups. The N–H stretching, which normally appears at about 3380 cm⁻¹, could not be discerned as it overlaid the strong broad band at \sim 3450 cm⁻¹ of the surface hydroxyl groups of the mesoporous SiO₂ [42].

3.3. Immobilization of GOx on mesoporous SiO₂ and functionalized mesoporous SiO₂

3.3.1. Mechanistic consideration

Physical adsorption is the simplest method of immobilizing enzyme onto ordered mesoporous SiO₂. Since there is no further

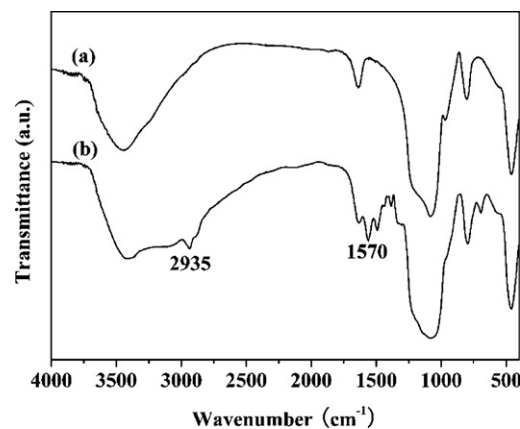
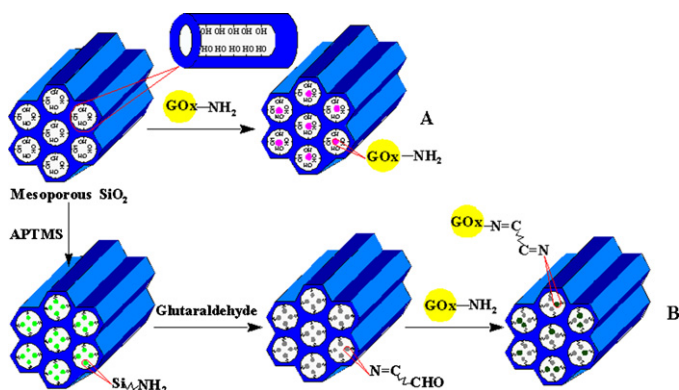


Fig. 2. FT-IR spectra of vesicle-like SiO₂ before (a) and after (b) modification with APTMS.



Scheme 1. The possible mechanisms of GOx immobilization onto the internal surfaces of mesoporous SiO₂ and functionalized mesoporous SiO₂. (A) Physisorption and (B) chemisorption.

treatment, denaturation of enzyme is avoided. Possible physical adsorption forces of GOx on mesoporous silica involved here include weak van der Waals interaction, hydrogen bonding interaction, and electrostatic interactions between the GOx molecules and silanol groups on the internal surface of the mesoporous materials [43].

After the successful amine functionalization, GOx was then covalently bound to the APTMS modified mesoporous SiO₂ using glutaraldehyde as the cross-linker. In the first step, the reaction between the hydroxyl groups of mesoporous SiO₂ and APTMS was performed; then the product of this reaction was treated with glutaraldehyde. In the third step, the superficial amino groups of the GOx were made to react with the functionalized support to produce the chemically adsorbed immobilization GOx on mesoporous SiO₂ [43,44]. Formation of covalent bonds with functionalized surfaces ensures strong binding and negligible leaching of enzyme. The possible mechanisms of GOx immobilization onto the internal surfaces of mesoporous SiO₂ and functionalized mesoporous SiO₂ by physisorption and chemisorption are shown in Scheme 1.

3.3.2. Nitrogen adsorption–desorption isotherms

The nitrogen adsorption–desorption isotherms of the rod-like and the vesicle-like SiO₂ are shown in Fig. 3, together with the resulting Barrett–Joyner–Halenda (BJH) pore size distributions determined from the corresponding adsorption branches, for the samples before and after loading of GOx. One can see that the amount of nitrogen adsorbed decreased markedly in the rod-like SiO₂ (from 687 to 413 cm³ g^{−1}) and the vesicle-like SiO₂ (from 874 to 533 cm³ g^{−1}) upon GOx adsorption. Similar results were reported previously by our group for the adsorption of lipase from *Candida rugosa* onto the mesoporous SiO₂ [12]. The nitrogen adsorption–desorption isotherms (Fig. 3A and B) of the rod-like SiO₂ before and after adsorption of GOx are of type IV with an H1-type hysteresis loop that is characteristic of SBA-15. In contrast, the sorption isotherms (Fig. 3C and D) of the vesicle-like SiO₂ before and after adsorption of GOx are different from a typical type IV of SBA-15. For instance, these sorption isotherms have a broad hysteresis loop in the range of $P/P_0 = 0.51–0.99$, which does not close until the saturation pressure is reached [12]. The specific surface areas and the total pore volumes of the rod-like and vesicle-like SiO₂ were also drastically reduced after GOx adsorption. For the rod-like SiO₂, the specific surface area was decreased from 437 to 299 m² g^{−1} and the total pore volume from 1.09 to 0.65 cm³ g^{−1}. More significant for the vesicle-like SiO₂, the adsorption of GOx led to the decrease of the specific surface area from 509 to 183 m² g^{−1} and the total pore volume reduction from 1.49 to 0.77 cm³ g^{−1}. These results indicate that the GOx molecules were

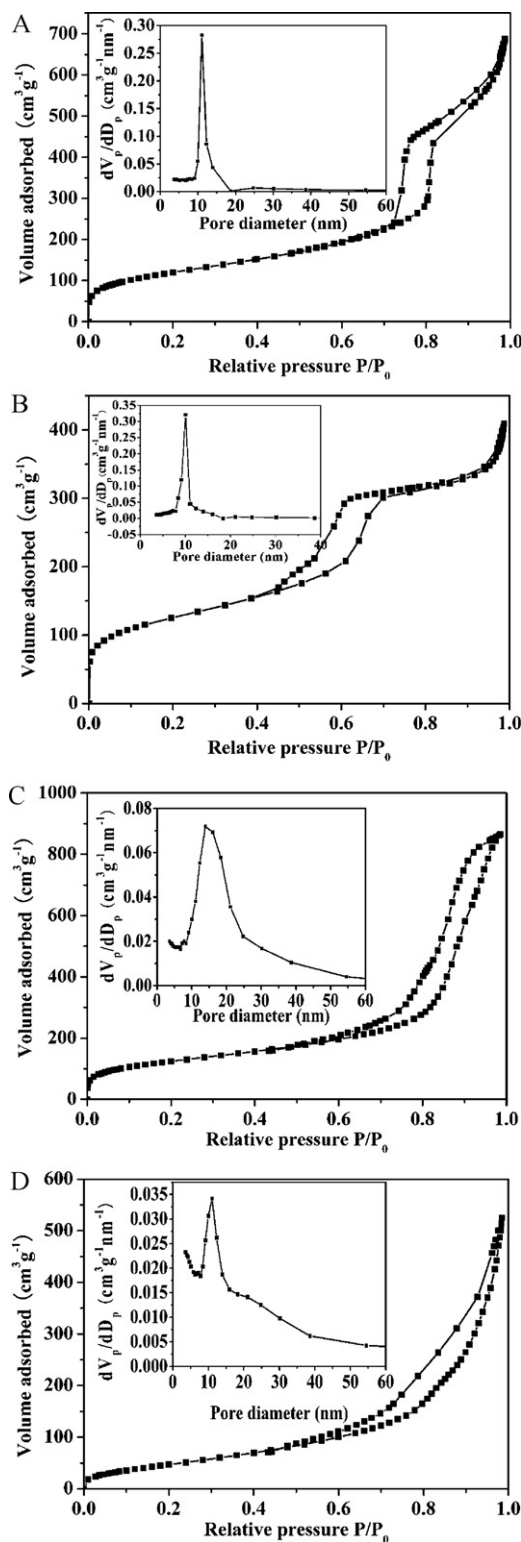


Fig. 3. N₂ adsorption–desorption isotherms and pore diameter distribution curves (insert) of rod-like SiO₂ before (A), after (B) GOx loading and vesicle-like SiO₂ before (C) and after (D) GOx loading.

adsorbed on the internal surfaces of the mesopores rod-like and vesicle-like SiO₂. The higher amount of GOx adsorbed on vesicle-like SiO₂ than on the rod-like silica is consistent with its higher specific surface area (509 m² g^{−1}) and larger total pore volume (1.49 cm³ g^{−1}).

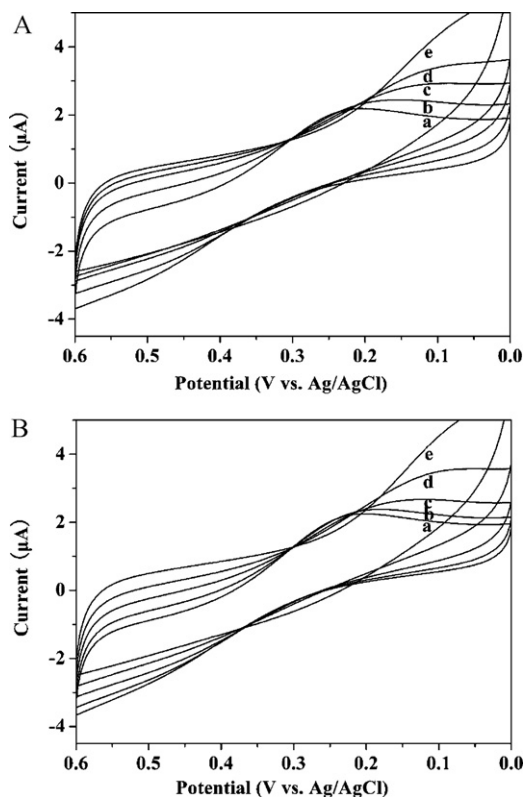
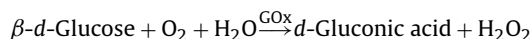


Fig. 4. The CV curves at different glucose concentration measured by rod-like mesoporous SiO₂ (A) or vesicle-like mesoporous SiO₂ (B) immobilized GOx modified electrode. The glucose concentrations were 0 mM (curve a), 2 mM (curve b), 4 mM (curve c), 8 mM (curve d) and 16 mM (curve e), respectively.

3.4. Electrochemical characterization of GOx modified electrode

3.4.1. Principle of the amperometric measurement

The amperometric glucose biosensors are based on the oxidation of glucose by according to the following reactions:



The amperometric sensors can respond to glucose by detecting the current generated by the oxidation of hydrogen dioxide on the electrode at +600 mV versus Ag/AgCl reference electrode. Higher glucose concentration and higher enzymatic activity will both lead to a higher rate of H₂O₂ production, and thus higher current response. The former agrees with the general trend of the data that the current responses of the enzyme-modified electrodes increase with the glucose concentration. The latter is reflected by the fact that the introduction of the mesoporous SiO₂ increases the current responses dramatically.

3.4.2. Cyclic voltammetric behavior of GOx modified electrode

CV measurement was done with a potential scan rate of 100 mV s⁻¹. The resulted CV curves with different concentrations (0, 2, 4, 8 and 16 mM) of glucose measured by the electrode modified with rod-like mesoporous SiO₂ or vesicle-like mesoporous SiO₂ immobilized GOx were shown in Fig. 4. Anodic peak current become stable at potential lower than +210 mV for rod-like mesoporous SiO₂ or vesicle-like mesoporous SiO₂ immobilized GOx modified electrode at glucose concentrations 0 and 2 mM. While at higher glucose concentrations (4, 8 and 16 mM), the cyclic voltammograms show that an obvious increase in anodic peak current with the glucose concentration increasing. The results show that the mesoporous SiO₂ immobilized GOx

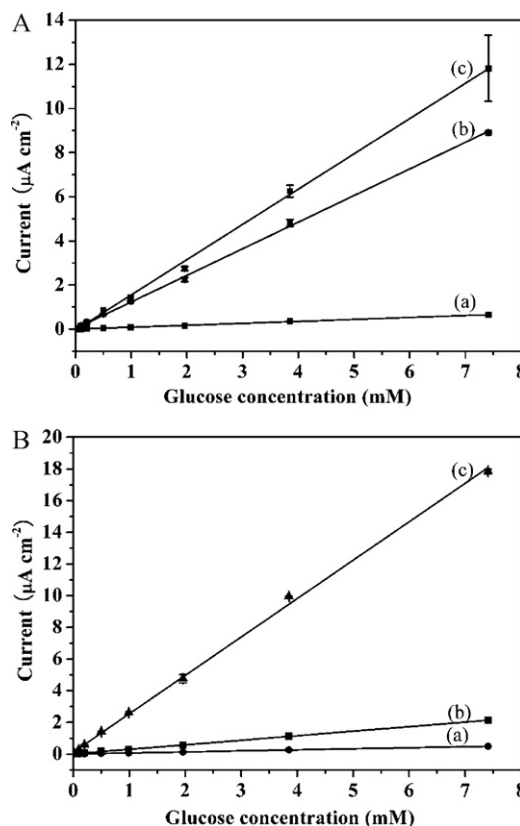


Fig. 5. Calibration plots of current versus glucose concentration for biosensors fabricated with rod-like SiO₂ (A) and vesicle-like SiO₂ (B). (a) GOx only, (b) mixture of GOx and mesoporous SiO₂, and (c) GOx physically adsorbed on mesoporous SiO₂.

modified electrode can be used as biosensor for measurement of glucose.

3.4.3. Current response of physisorbed GOx modified electrode

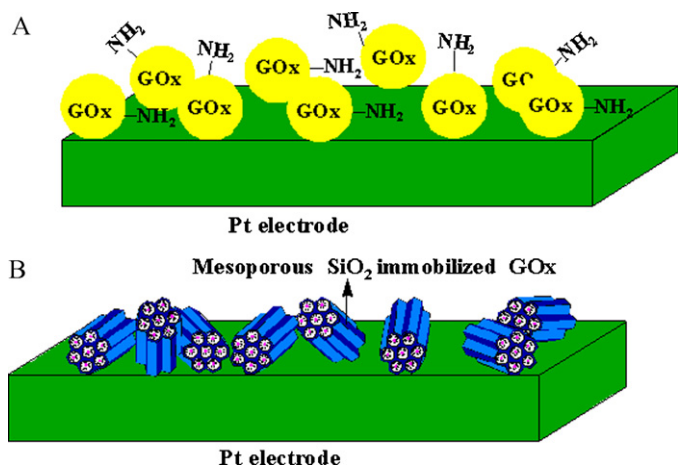
In this study, we investigated the effect of different morphologies of mesoporous SiO₂ other than SiO₂ sphere, namely rod-like and vesicle-like mesoporous SiO₂, on the performance of the glucose biosensors. The current responses of the electrodes of Pt/GOx, Pt/GOx mixed with rod-like and vesicle-like mesoporous SiO₂, and Pt/GOx immobilized on rod-like and vesicle-like mesoporous SiO₂ were tested by using a Biometra EP-30 potentiostat. Fig. 5 shows the current responses of these electrodes. The results clearly show that the current responses of the enzyme electrodes increase with the glucose concentration and more important, the current responses of the mesoporous SiO₂ containing enzyme electrodes increase dramatically. Particularly interesting is the observation that all of the current responses for the electrodes with the enzymes immobilized on the mesoporous SiO₂ are significantly higher than those modified by simply mixing the GOx and the mesoporous SiO₂. It appears that GOx immobilization onto the mesoporous silica tends to maximize the enzymatic activity. As can also be seen from Fig. 5A and B, the linear response range of the sensor responses to the glucose concentration can extend to at least 7.5 mM. Tables 1 and 2 summarize the sensitivity, linear range and detection limit of glucose biosensors using rod-like SiO₂ and vesicle-like SiO₂ as hosts for GOx with different immobilization strategies, respectively. The response sensitivities and the detection limits of the GOx biosensors prepared using different enzyme immobilization strategies are 1.60 μA mM⁻¹ cm⁻², 3.2 μA mM⁻¹ cm⁻² and 2.42 μA mM⁻¹ cm⁻², 1.6 μA mM⁻¹ cm⁻² for GOx physisorbed on rod-like SiO₂ and GOx physisorbed on vesicle-like SiO₂, respectively. The greater response enhancement of the electrodes modified using GOx immobilized in the vesicle-like SiO₂

Table 1The sensitivity, linear range and detection limit of glucose biosensors using rod-like SiO₂ as hosts for GOx with different immobilization strategies.

Modified electrodes	Sensitivity ($\mu\text{A mM}^{-1} \text{cm}^{-2}$)	Linear range (mM)	Detection limit (μM)
GOx only (control)	0.09	0.1–7.5	10.9
GOx and rod-like SiO ₂ mixture	1.21	0.02–7.5	3.2
GOx physisorbed on rod-like SiO ₂	1.60	0.01–7.5	3.2

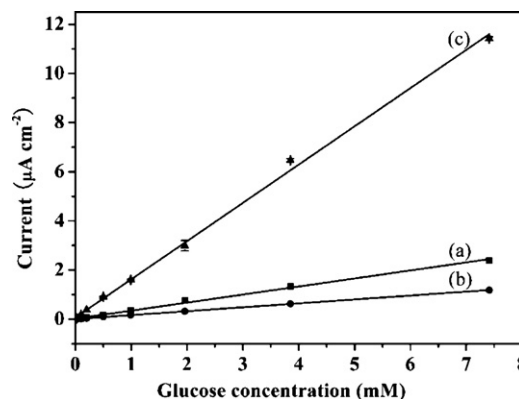
Table 2The sensitivity, linear range and detection limit of glucose biosensors using vesicle-like SiO₂ as hosts for GOx with different immobilization strategies.

Modified electrodes	Sensitivity ($\mu\text{A mM}^{-1} \text{cm}^{-2}$)	Linear range (mM)	Detection limit (μM)
GOx only (control)	0.07	0.1–7.5	25.6
GOx and vesicle-like SiO ₂ mixture	0.29	0.02–7.5	13.5
GOx physisorbed on vesicle-like SiO ₂	2.42	0.01–7.5	1.6

**Scheme 2.** Schematic representation of platinum electrodes modified with free GOx (A) and modified with mesoporous SiO₂ immobilized GOx (B).

can be ascribed to its peculiar pore surfaces, higher specific surface area ($509 \text{ m}^2 \text{g}^{-1}$) and larger total pore volume ($1.49 \text{ cm}^3 \text{g}^{-1}$). These results give similar sensor performance to that reported by Yang and Zhu, who modified Pt electrode with SiO₂ nanoparticles immobilized GOx [28].

As mentioned above, the current responses for the electrodes with the enzymes immobilized on the mesoporous SiO₂ are significantly higher than those modified by simply mixing the GOx and the mesoporous SiO₂. This is true for both the rod-like and the vesicle-like mesoporous SiO₂. Since the amount of active GOx on all the electrodes for a given type of mesoporous SiO₂ was the same, this result suggests that the role of the mesoporous SiO₂ is not only to increase the surface area for enzyme loading, but also to preserve and/or enhance the enzyme activity by keeping the enzymes in a favorable folding conformation for catalysis, which led to the further improvement in sensitivity. For immobilized enzyme, some hydration water can be retained between the adsorbed enzyme layer and its interface with the mesoporous SiO₂, helping to form highly hydrated enzyme molecules. As a result, the immobilized enzyme onto the mesoporous SiO₂ would show a higher intrinsic activity than free enzyme [12,45]. This is because the co-factor

**Fig. 6.** Calibration plots of current versus glucose concentration for biosensors fabricated with (a) GOx only, (b) a mixture of GOx and vesicle-like SiO₂-NH₂, and (c) GOx covalently bound on vesicle-like SiO₂-NH₂.

flavin-adenine dinucleotide (FAD), the polar part normally buried in the interior of the enzyme, can then become exposed to the water, which can increase the activity of the immobilized enzyme [46]. The proposed mechanisms for platinum electrodes modified with free GOx and modified with mesoporous SiO₂ immobilized GOx are shown in Scheme 2.

3.4.4. Current response of chemisorbed GOx modified electrode

After the successful amine functionalization, GOx was then covalently bound to the APTMS modified mesoporous SiO₂ using glutaraldehyde as the cross-linker. Fig. 6 shows the current responses of such electrodes (Fig. 6c), together with those of free GOx electrodes (Fig. 6a) and of mixtures of GOx and vesicle-like SiO₂-NH₂ (Fig. 6b). One can see that the current responses of the electrodes modified using GOx covalently bound on the vesicle-like SiO₂-NH₂ are higher than those of the electrodes modified using the mixture of GOx and the vesicle-like SiO₂-NH₂. The data for the amperometric response sensitivity, linear range and detection limit of the GOx biosensors using vesicle-like SiO₂-NH₂ with different enzyme immobilization strategies are charted in Table 3.

It should be pointed out that although the glucose biosensor with GOx covalently bound to the vesicle-like SiO₂-NH₂

Table 3The sensitivity, linear range and detection limit of glucose biosensors using vesicle-like SiO₂-NH₂ as a host for GOx with different immobilization strategies.

Modified electrodes	Sensitivity ($\mu\text{A mM}^{-1} \text{cm}^{-2}$)	Linear range (mM)	Detection limit (μM)
GOx only (control)	0.33	0.05–7.5	10.8
GOx and vesicle-like SiO ₂ -NH ₂ mixture	0.16	0.1–7.5	14.4
GOx chemisorbed on vesicle-like SiO ₂ -NH ₂	1.56	0.01–7.5	5.2

resulted in a higher enzyme loading, it showed a lower sensitivity ($1.56 \mu\text{A mM}^{-1} \text{cm}^{-2}$) than the one ($2.42 \mu\text{A mM}^{-1} \text{cm}^{-2}$) with physisorbed GOx. A possible explanation for this seemingly counterintuitive result is related to the type of covalent bond between the mesoporous vesicle-like SiO_2 and the GOx molecules, which could compromise the enzyme flexibility. In other words, the strong covalent interactions between the vesicle-like $\text{SiO}_2\text{-NH}_2$ and GOx may restrict the self-dynamics of the bound enzyme molecules required for catalytic sensitivity. Furthermore, it may also distort the tertiary structure of the enzyme with its consequent partial inactivation [40]. On the contrary, in the physisorption case, the weak physical interactions between the vesicle-like SiO_2 and GOx are likely to preserve the active conformation of the enzyme, thus favoring the high catalytic sensitivity, despite the low loading.

4. Conclusions

We have conducted a comparative study on the immobilization of GOx in rod-like and vesicle-like mesoporous silica for the development of glucose biosensors. We have shown that the mesoporous structure remained rod-like for the hexagonal channels and vesicle-like for the multilamellar channels after GOx immobilization. The mesoporous rod-like and vesicle-like SiO_2 were used to immobilize GOx by physisorption and by covalent linkage to fabricate a series of glucose biosensors. The electrodes modified with GOx immobilized in the mesoporous rod-like and vesicle-like SiO_2 have demonstrated high potential for glucose detection; much higher bioelectrocatalytic activity was observed with GOx immobilized on the mesoporous SiO_2 than free GOx. We have also shown the effect of the morphologies of the mesoporous SiO_2 on the sensitivity of the surface-modified glucose biosensors. Namely, the glucose biosensors with GOx covalently bound on the vesicle-like $\text{SiO}_2\text{-NH}_2$ have a lower sensitivity than those with the physisorbed GOx due possibly to the altered static and dynamic conformations. The results of this study should be helpful for the development of high performance glucose biosensors and biosensors in general.

Acknowledgments

This work was supported by the Hong Kong RGC General Research Fund (JRF no. 604608), the National Natural Science Foundation of China (Grant no. 20976100) and the Natural Science Foundation of Shandong Province (Grant no. ZR2010BM013).

References

- [1] C.T. Kresge, M. Leonowicz, W.J. Roth, J.C. Vartuli, J.S. Beck, *Nature* 359 (1992) 710–712.
- [2] D. Zhao, P. Yang, B.F. Chmelka, G.D. Stucky, *Chem. Mater.* 11 (1999) 1174–1178.

- [3] Z. Liang, A.S. Susha, *Chem. Eur. J.* 10 (2004) 4910–4914.
- [4] X. Wu, J. Ruan, T. Ohsuna, O. Terasaki, S. Che, *Chem. Mater.* 19 (2007) 1577–1583.
- [5] G. Zhou, Y. Chen, J. Yang, S. Yang, *J. Mater. Chem.* 17 (2007) 2839–2844.
- [6] D. Niu, Z. Ma, Y. Li, J. Shi, *J. Am. Chem. Soc.* 132 (2010) 15133–15147.
- [7] C. Ispas, I. Sokolov, S. Andreescu, *Anal. Bioanal. Chem.* 393 (2009) 543–554.
- [8] J.F. Diaz, K.J. Balkus, *J. Mol. Catal. B* 2 (1996) 115–126.
- [9] X. Zhang, R.F. Guan, D.Q. Wu, K.Y. Chan, *J. Mol. Catal. B: Enzym.* 33 (2005) 43–50.
- [10] Y. Han, S.S. Lee, J.Y. Ying, *Chem. Mater.* 18 (2006) 643–649.
- [11] M. Mureseanu, A. Galarneau, G. Renard, F. Faula, *Langmuir* 21 (2005) 4648–4655.
- [12] G. Zhou, Y. Chen, S. Yang, *Micropor. Mesopor. Mater.* 119 (2009) 223–229.
- [13] J.L. Blin, C. Cerardin, C. Carteret, L. Rodehuser, C. Selve, M.J. Stebe, *Chem. Mater.* 17 (2005) 1479–1486.
- [14] X. Zhong, R. Yuan, Y. Chai, Y. Liu, J. Dai, D. Tang, *Sens. Actuators B* 104 (2005) 191–198.
- [15] D. Feng, F. Wang, Z. Chen, *Sens. Actuators B* 138 (2009) 539–544.
- [16] S. Guo, D. Wen, S. Dong, E. Wang, *Talanta* 77 (2009) 1510–1517.
- [17] H. Wang, X. Wang, X. Zhang, X. Qin, Z. Zhao, Z. Miao, N. Huang, Q. Chen, *Biosens. Bioelectron.* 25 (2009) 142–146.
- [18] S. Zhang, N. Wang, Y. Niu, C. Sun, *Sens. Actuators B* 109 (2005) 367–374.
- [19] X. Wen, Y.T. Xie, M.W.C. Mak, K.Y. Cheung, X.Y. Li, R. Renneberg, S. Yang, *Langmuir* 22 (2006) 4836–4842.
- [20] M.S.M. Quintino, K. Araki, H.E. Toma, L. Agnes, *Talanta* 74 (2008) 730–735.
- [21] W. Ngeontae, W. Janrungroatsakul, P. Maneewattanapinyo, S. Ekgsit, W. Aeungmaitrepirom, T. Tuntulani, *Sens. Actuators B* 137 (2009) 320–326.
- [22] F. Miao, B. Tao, L. Sun, T. Liu, J. You, L. Wang, P.K. Chu, *Sens. Actuators B* 141 (2009) 338–342.
- [23] Y. Liu, M. Wang, F. Zhao, Z. Xu, S. Dong, *Biosens. Bioelectron.* 21 (2005) 984–988.
- [24] Y.C. Tsai, S.C. Li, S.W. Liao, *Biosens. Bioelectron.* 22 (2006) 495–500.
- [25] G.D. Withey, A.D. Lazarek, M.B. Tzolov, A. Yina, P. Aich, J.I. Yeh, J.M. Xua, *Biosens. Bioelectron.* 21 (2006) 1560–1565.
- [26] I. Capek, *Adv. Colloid Interface Sci.* 150 (2009) 63–89.
- [27] F.F. Zhang, Q. Wan, X.L. Wang, Z.D. Sun, Z.Q. Zhu, Y.Z. Xian, L.T. Jin, K. Yamamoto, *J. Electroanal. Chem.* 571 (2004) 133–138.
- [28] H. Yang, Y. Zhu, *Talanta* 68 (2006) 569–574.
- [29] L. Zhang, S. Dong, *Anal. Chem.* 78 (2006) 5119–5123.
- [30] W. Xue, T. Cui, *Sens. Actuators B* 134 (2008) 981–987.
- [31] X. Ren, X. Meng, F. Tang, L. Zhang, *Mater. Sci. Eng. C* 29 (2009) 2234–2238.
- [32] D. Lee, J. Lee, J. Kim, J. Kim, H.B. Na, B. Kim, C.H. Shin, J.H. Kwak, A. Dohnalkova, J.W. Grate, T. Hyeon, H.S. Kim, *Adv. Mater.* 17 (2005) 2828–2833.
- [33] H. Yang, Y. Zhu, *Anal. Chim. Acta* 554 (2005) 92–97.
- [34] X.L. Luo, J.J. Xu, W. Zhao, H.Y. Chen, *Sens. Actuators B* 97 (2004) 249–255.
- [35] Z. Dai, X. Xu, L. Wu, H. Ju, *Electroanalysis* 17 (2005) 1571–1577.
- [36] T. Shimomura, T. Itoh, T. Sumiya, F. Mizukami, M. Ono, *Sens. Actuators B* 135 (2008) 268–275.
- [37] F. Pereira, K. Vallé, A. P/Belleville, S. Morin, C. Lambert, Sanchez, *Chem. Mater.* 20 (2008) 1710–1718.
- [38] Y. Piao, D. Lee, J. Lee, T. Hyeon, J. Kim, H.S. Kim, *Biosens. Bioelectron.* 25 (2009) 906–912.
- [39] Y.X. Bai, Y.F. Li, Y. Yang, L.X. Yi, *Process Biochem.* 41 (2006) 770–777.
- [40] A. Salis, M.S. Bhattacharyya, M. Monduzzi, V. Solinas, *J. Mol. Catal. B: Enzym.* 57 (2009) 262–269.
- [41] E. Gianotti, V. Dellarocca, L. Marchese, G. Martra, S. Coluccia, T. Maschmeyer, *Phys. Chem. Chem. Phys.* 4 (2002) 6109–6115.
- [42] Q. Wei, Z.R. Nie, Y.L. Hao, L. Liu, Z.X. Chen, J.X. Zou, *J. Sol-Gel Sci. Technol.* 39 (2006) 103–109.
- [43] H.H.P. Yiu, P.A. Wright, *J. Mater. Chem.* 15 (2005) 3690–3700.
- [44] A. Salis, D. Meloni, S. Ligas, M.F. Casula, M. Monduzzi, V. Solinas, E. Dumitriu, *Langmuir* 21 (2005) 5511–5516.
- [45] B. Wu, G. Zhang, S. Shuang, M. Choi, *Talanta* 64 (2004) 546–553.
- [46] Z. Chen, X. Ou, F. Tang, L. Jiang, *Colloids Surf. B* 7 (1996) 173–179.